Nonequilibrium effects in the proton neutral fraction emerging from solids bombarded with MeV H^0, H^+, H_2^+, and H_3^+ beams

M. J. Gaillard, J. C. Poizat, A. Ratkowski,* J. Remillieux, and M. Auzas

Institut de Physique Nucléaire (IN2P3), Université Claude Bernard Lyon-1, 43, Bd du 11 Novembre 1918, 69621 Villeurbanne, France
(Received 9 May 1977)

We have investigated nonequilibrated neutral fractions in hydrogen beams transmitted through carbon foils bombarded with H^0, H_2^+, and H_3^+ projectiles having energies from 0.5 to 2.4 MeV/amu. Measurements with neutral projectiles provide a direct determination of the charge-exchange cross sections for fast protons in solids. The fact that the solid cross sections have been found close to the corresponding gas cross sections is discussed and confronted with existing theories. For very short dwell times the role played by projectile electrons in neutral-atom production is demonstrated, and it is shown that the approach to equilibrium follows essentially the same law for H^0, H_2^+, and H_3^+ projectiles. An overproduction of neutrals has also been observed with molecular ion projectiles for longer dwell times. An explanation of this effect is suggested in terms of a multistep process in which a target electron gets correlated with one proton before being captured by another proton of the cluster. Angular distributions of neutrals produced from incident molecular beams indicate the possible formation of a repulsive molecular state on emergence from the foil.

I. INTRODUCTION

Transmission measurements in which protons are incident upon gaseous and solid targets reveal hydrogen atoms in the emerging beam, the neutral fraction Φ_0 having been extensively studied in the former case. Recently, increasing interest in the neutral fraction in beams emerging from thin solid targets has been manifested by both experimentalists[1,2] and theoreticians.[3,4] The focus of these studies was determination of the dependence of the equilibrated neutral fraction on both projectile velocity v_1 and target atomic number Z_2, and comparison with theory, which predicts the high-velocity equilibrated neutral fraction to be the ratio of the electron capture and loss cross sections σ_c and σ_l. Following the arguments of Brandt,[5] protons could not bind an electron inside a solid; σ_c and σ_l are then the cross sections for gain and loss of correlation between the projectiles and target electrons. The mean free path of this correlation inside the solid is usually very small compared with the target thickness, and for incident H^+ beams, only the equilibrated neutral fraction can easily be measured. However, nonequilibrated charge distributions were observed[1] for 7-MeV H^+ bombarding Ag and Au foils thinner than 500 Å.

In addition, bulk effects have been observed in channeling experiments.[2] It has been shown that channeling conditions lead to an equilibrium corresponding to a lower neutral fraction when the proton velocity is comparable with the velocities of the target core electrons. This channeling effect on the charge states was interpreted as a reduced probability for capturing a target core electron. In fact, this effect must be related to the reduction of the neutral fraction observed in the same velocity range with amorphous foils of decreasing atomic number Z_2; as an example, a 2-MeV proton beam channeled along the $\langle 110 \rangle$ axis of a 1200 -Å-thick gold crystal ($Z_2 = 79$) gives about the same neutral fraction as if it had emerged from an amorphous carbon foil ($Z_2 = 6$).

Another type of nonequilibrated charge distribution has been observed when foils are bombarded with molecular beams. The fact that molecular beams can produce more neutral atoms than atomic beams of the same velocity was first reported by Meggitt et al.[6]; in the energy range 100–150 keV/amu, H_2^+ molecular beams produce about 40% more neutrals emerging from a 5-μg/cm² carbon foil. They also observed that this effect decreases to about 20% when the foil thickness increases to 10 μg/cm². Similar trends were also observed at higher energies by Chateau-Thierry and Gladieux.[7]

The purpose of this paper is a systematic study of the neutral fraction emerging from amorphous carbon foils bombarded by various hydrogen species (H^+, H^0, H_2^+, and H_3^+) having energies from 0.5 to 2.4 MeV/amu. In Sec. II we give a description of the experimental method. In Sec. III we describe the nonequilibrated neutral fractions measured with neutral projectiles. These measurements provide a direct determination of charge-exchange cross sections in solids. These cross sections are then compared with existing theories and measurements.

In Sec. IV we analyze the production of neutrals from a proton cluster. The observed overproduction of neutrals exhibits a short-dwell-time behavior which is clearly due to the role played by

the molecular electrons injected with the incident H_2^+ and H_3^+ projectiles. These results are interpreted in the framework of the conclusions of Sec. III. The long-dwell-time behavior of the observed overproduction of neutrals is tentatively explained by an increase of the capture probability of correlated electrons emerging with the cluster.

In Sec. V we study the angular distributions of neutrals produced from a cluster and consider the possible formation of an unstable H_2^+ molecular system.

II. EXPERIMENTAL METHOD

Experimental problems related to measurement of the emerging neutral fraction are (i) the production of an uncontaminated low-intensity beam of H^0, H_2^+, and H_3^+ projectiles, (ii) the measurement of the thickness, the uniformity, and the density of the carbon foil targets, and (iii) the collection, downstream from the foil, of all the transmitted particles emerging as protons and neutrals, a condition which requires detectors having large acceptance angles.

Three different configurations have been used to measure (a) the neutral fraction in the total trans-

mitted beam for incident atomic projectiles (H^+ or H^0), (b) the neutral fraction in the total transmitted beam for incident molecular projectiles (H_2^+ or H_3^+), and (c) the angular distribution of the emerging neutral and charged components for incident atomic and molecular projectiles.

Hydrogen-ion beams were obtained from the 2.5-MeV Van de Graaff accelerator at the Institut de Physique Nucléaire de Lyon.

A. Measurements of Φ_0 with H^0 beams

The experimental arrangement is shown in Fig. 1(a). The incident proton beam is collimated to $\pm 0.016°$ by two circular apertures D_1 and D_2. A thin carbon foil is then inserted into the charged beam, immediately behind the collimator D_1. In the velocity range considered, the foil neutralizes 3×10^{-4} to 3×10^{-5} of the incident projectiles. The charged component of the transmitted beam is removed by means of a permanent magnet inserted between collimators D_1 and D_2. The energy spread introduced by the neutralizing foil is negligible. The charged fraction emerging from the carbon target is magnetically separated from the neutrals
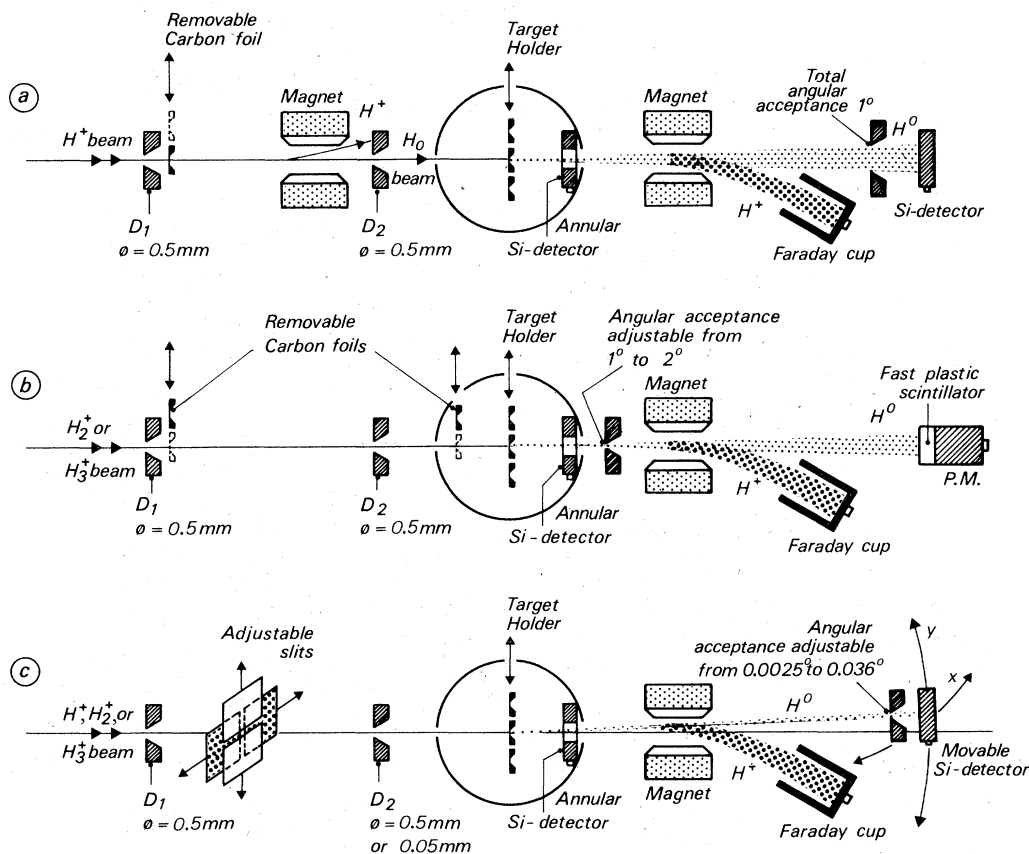
FIG. 1. Experimental arrangement employed to measure (a) Φ_0 with an incident neutral beam. (b) Φ_0 with an incident molecular beam, and (c) angular distributions of protons and neutrals emerging from a target.

which are detected in a silicon surface-barrier detector which has a total angular acceptance of 1°. Measurements are monitored by the number of protons forward scattered by the target into an annular silicon surface-barrier detector located in the target chamber and aligned on the transmitted beam. The scattering yield in the annular detector, per incident proton, was first determined in a preliminary measurement with higher beam intensity.

B. Measurement of Φ_0 with H^+, H_2^+, and H_3^+ beams

The experimental arrangement is shown in Fig. 1(b). As will be explained later, the angular distributions of emerging neutrals and protons are quite different if the incident projectile is a molecule or an atom. It is necessary to measure the charge distribution within a large angular acceptance to be certain that the entire transmitted beam is properly collected. Previous reports of similar measurements performed by other workers were not explicit enough to let the reader know whether this condition was fulfilled.

In our measurement, the large angular acceptance of the detectors was obtained by using a Faraday cup to detect the protons and a fast plastic scintillator to detect the neutrals. The scintillator was of the NE 810 type, 38 mm in diameter, and was attached to an XP 1020 photomultiplier tube. This allowed angular acceptances up to 2° and counting rates up to 10^5 s^{-1}. The beam intensity was typically 0.1 to 10 pA.

In this configuration, a thin carbon foil could be inserted into the incident beam to dissociate molecular ion projectiles into free protons. This method was used to compare the H production with molecular and atomic projectiles of equal velocity in identical geometrical conditions. The composition of incident molecular ion beams was carefully verified to avoid a mixing of molecular ions and dissociation products (H^+ and H^0) resulting from collisions with collimator edges and residual gas atoms. This was achieved by directly measuring the composition of the incident beam when the target was removed. In this experiment, the beam current was measured with a beam chopper located at the entrance of the target chamber and compared with the current measured in the Faraday cup when the magnetic field was set to deflect the protons coming from dissociated molecular ions. In all cases, the fraction of dissociated projectiles was always lower than a few percent.

C. Measurement of the angular distribution of neutrals [Fig. 1 (c)]

Angular scans were performed by moving a tightly-collimated silicon surface-barrier detec-

tor through the neutral component of the transmitted beam after magnetic separation. The detector had an angular acceptance of 2.5 to 36×10^{-3} deg and was moved by stepping motors along lines perpendicular to the beam axis. The beam axis was determined by removing the target and scanning the incident beam. The corresponding proton distributions were measured by reducing the magnetic field in the magnet to zero.

Such angular scans clearly need very low beam currents to avoid pile-up in the particle detector. This was achieved by two pairs of mutually-perpendicular adjustable slits located between the collimators D_1 and D_2; it was possible to reduce the incident beam from a flux of a few nA to 10^3 projectiles per second. When these slits were used with molecular ion beams, it was necessary to carefully center the slits on the beam axis to prevent the few protons resulting from dissociation events (and located mainly at the periphery of the molecular beam) from entering the target chamber.

D. Target preparation and control

In order to calculate the dwell time of the projectiles in the target, one must know the volume density of the films. As this density may vary according to preparation techniques, the few data published in the literature about self-supporting carbon films[8] do not necessarily apply here. We measured the absolute thickness of our films by an interferometric method. Using the surface density determined from the Rutherford scattering experiment, we found that the volume density was $d = 1.65 \pm 0.15$ g/cm^3. The uncertainty quoted includes errors in both the scattering and optical measurements. This 10% uncertainty in the film thickness (or projectile dwell time) does not include the possibility of carbon buildup during the experiment for very thin targets. The target chamber was pumped by a turbomolecular pump and typical pressures during our measurements were of the order of 10^{-6} Torr.

III. NEUTRAL FRACTIONS FROM AN INCIDENT NEUTRAL BEAM

A. Introduction

In gas targets, charge-exchange cross sections are relatively easy to measure and are theoretically well-defined. With a solid target, the situation is more ambiguous because the emerging charge state of a projectile probably results from different processes occurring in the bulk and at the surface. Even with a projectile as simple as a proton, a swift neutral atom emerging from a

solid was considered by Brandt and Sizmann[3] to result from two processes: the first occurs inside the solid and is a collision in which a target electron gains correlation in speed and direction with the moving proton; the second occurs at the exit surface, if the correlation has not been lost, with the proton capturing the electron into a bound state. An experimental determination of the cross section for this multistep process can be achieved by studying nonequilibrated charge distributions. This method was employed, for instance, by Datz *et al.*[9] for channeled oxygen ions in gold crystals.

For MeV proton beams, the electron-loss cross section is too high to allow measurements of nonequilibrated distributions with self-supporting films because the equilibrated distribution is too close to the incident one. The purpose of this experiment was to introduce incident projectiles in a charge state as far as possible from the equilibrated distribution. Nonequilibrated distributions were clearly observed in transmission experiments by bombarding carbon films with hydrogen atoms.

B. Results

The experimental arrangement employed to produce a neutral incident beam and to measure the neutral fraction in the transmitted beam is described in Sec. II A. Neutral fractions Φ_0 have been measured for 1.2, 1.8, and 2.4 MeV H^0 beams transmitted through 2–10-μg/cm^2 carbon foils. The results are shown in Fig. 2 as a function of the dwell time t spent by the projectiles inside the foils.

For dwell times greater than 4×10^{-5} s, the charge distribution is clearly equilibrated and $\Phi_0(t)$ reaches the value $\Phi_0(\infty)$ measured with proton beams having the same velocity penetrating the same foils. $\Phi_0(\infty)$ is only dependent upon the projectile velocity v_1. In the range of velocities and thicknesses discussed here, the slowing down of the projectiles in the target is negligible. The data shown as $\Phi_0(\infty)$ in Fig. 2 have not been measured in the geometry described here with H^0 projectiles, but with an incident proton beam.

For shorter dwell times, Φ_0 increases strongly, and for dwell times less than 1.5×10^{-15}s, Φ_0 becomes dependent on v_1 only through an exponential dependence upon dwell time. For instance, with 2.4-MeV H^0 projectiles and $t = 0.8 \times 10^{-15}$ s the neutral fraction is three orders of magnitude higher than the equilibrated value.

Each measurement for a given foil was made for three different tilt angles (0°, 30°, and 45°) between the beam axis and the normal to the foil. The systematic agreement observed within the
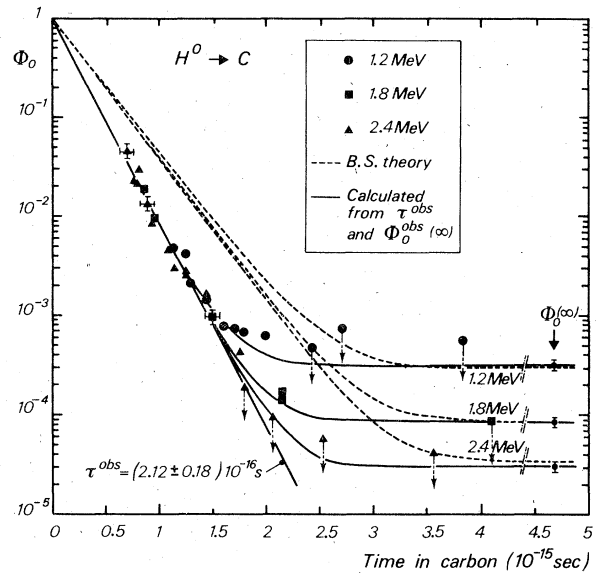
FIG. 2. Emerging neutral fraction Φ_0 as a function of the projectile dwell time in the foil for 1.2-, 1.8-, and 2.4- MeV H^0 beams bombarding 2–10-μg/cm^2 carbon foils. Arrows pointing downward indicate that only upper limits could be determined for the neutral fractions. Solid lines correspond to Eq. (5) calculated with the experimental values τ^{obs} and Φ_0^{obs} (∞). Dashed lines correspond to Eq. (5) calculated with the theoretical cross sections derived by Brandt and Sizmann.

experimental uncertainty in the Φ_0 values measured for a given dwell time realized with different foils and different tilt angles suggests two conclusions: firstly, if any tilt effect exists in the neutral production it is not observable here, and secondly, our targets are uniform in thickness and are free of holes.

C. Deduction of absolute charge-exchange cross sections and discussion

Our measurements for dwell times less than 1.5×10^{-15} s exhibit an exponential decrease of Φ_0 with time, compatible with the extrapolation to zero thickness that Φ_0 approaches unity when the dwell time approaches zero.

One can determine the time characteristic of this exponential decrease τ^{obs}, and obtain the electron-loss cross section σ_l from

$$\sigma_l = (N \, \tau^{obs} \, v_1)^{-1} , \qquad (1)$$

where N is the number of target atoms per unit volume.

The fact that τ^{obs} is independent of v_1 within experimental error shows that σ_l is essentially proportional to v_1^{-1} in our velocity range, a result predicted by Bohr to hold rigorously for light ions in

matter.

Let $f_1(x)$ and $f_0(x)$ be the proton and neutral fractions after thickness x of a target in which the cross sections for electron loss and electron capture are respectively σ_l and σ_c. A standard calculation gives the charged and neutral fractions:

$$f_1(x) = [\sigma_l/(\sigma_l + \sigma_c)] + [f_1(0) - \sigma_l/(\sigma_l + \sigma_c)]$$
$$\times \exp[-(\sigma_l + \sigma_c)Nx] \qquad (2)$$

and

$$f_0(x) = [\sigma_c/(\sigma_l + \sigma_c)] + [f_0(0) - \sigma_c/(\sigma_l + \sigma_c)]$$
$$\times \exp[-(\sigma_l + \sigma_c)Nx], \qquad (3)$$

where $f_1(0)$ and $f_0(0)$ are the charged and neutral fractions in the incident beam.

The equilibrated neutral fraction is $\Phi_0(\infty) = f_0(\infty)$ $= \sigma_c/(\sigma_l + \sigma_c)$. For MeV projectiles, $\sigma_c \ll \sigma_l$ and $\Phi_0(\infty) \sim \sigma_c/\sigma_l \ll 1$. For neutral projectiles $f_0(0) = 1$, and (3) becomes

$$f_0(x) \sim \Phi_0(\infty) + [1 - \Phi_0(\infty)]\exp(-\sigma_l Nx) \qquad (4)$$

or, after introducing the projectile dwell time $t = x/v_1$ and the "electron lifetime" $\tau = (N\sigma_l v_1)^{-1}$,

$$\Phi_0(t) \sim \Phi_0(\infty) + [1 - \Phi_0(\infty)]\exp(-t/\tau) \qquad (5)$$

describing the variation of Φ_0 with the dwell time observed in Fig. 2. The solid lines correspond to Eq. (5) calculated with the experimental values

$$\tau = \tau^{\mathrm{obs}} = 2.12 \times 10^{-16}\ \mathrm{s}$$

and

$$\Phi_0(\infty) = \Phi_0^{\mathrm{obs}}(\infty) = \begin{cases} 3.1 \times 10^{-4} & \text{at } 1.2\ \text{MeV}, \\ 8.7 \times 10^{-5} & \text{at } 1.8\ \text{MeV}, \\ 3.0 \times 10^{-5} & \text{at } 2.4\ \text{MeV}. \end{cases}$$

The dotted lines correspond also to Eq. (5), but the cross sections employed are those derived by Brandt and Sizmann[1] (BS) for protons inside a solid target of atomic number Z_2,

$$\sigma_c^{\mathrm{BS}} = \pi a_0^2 (2^{18}/5)Z_2^5 v_1^{-6}(v_1^2 + 2^6 \times 40^{-1/3} \times Z_2^{14/9})^{-3} \qquad (6)$$

and

$$\sigma_l^{\mathrm{BS}} = \pi a_0^2 \frac{Z_2^{2/3}}{Z_2^{2/3} + v_1} \frac{4Z_2^{1/3}(Z_2+1)}{4Z_2^{1/3}(Z_2+1) + v_1}, \qquad (7)$$

where a_0 is the Bohr radius, and v_1 is the proton velocity in atomic units.

These theoretical cross sections were already known as being in good agreement with the equilibrated neutral fraction $\Phi_0(\infty)$ over a large velocity range. But our work reveals a systematic deviation in the description of the nonequilibrated neutral fraction which depends not only on the ratio σ_c/σ_l but on the absolute values of these cross sections as well.

The absolute values can be calculated from τ^{obs} and $\Phi_0^{\mathrm{obs}}(\infty)$: $\sigma_l^{\mathrm{obs}} = (Nv_1\tau^{\mathrm{obs}})^{-1}$, and $\sigma_c^{\mathrm{obs}} = \sigma_l^{\mathrm{obs}}\Phi_0^{\mathrm{obs}}(\infty)$. Table I gives a comparison between these experimental values and the Brandt-Sizmann cross sections; the experimental cross sections for loss and capture are both higher than predicted by this theory.

It is of interest to compare these data with gas target values. Although no direct measurement exists for carbon targets in the gas phase, Toburen et al.[10] gave an indirect determination of σ_l and σ_c by applying an additivity rule to the cross sections of each compound from measurements in various carbon-containing gas targets (CO_2, CH_4, C_2H_4, C_2H_6, and C_4H_{10}). The result of their calculation of σ_l and σ_c in our energy range is shown in Fig. 3. When comparing our data with the indirect measurements of Toburen et al. in gases and the prediction of Brandt and Sizmann in solid carbon, we conclude that, to the extent that the additivity rule is applicable, the MeV energy-range cross sections for charge exchange are nearly the same in solid carbon, and for carbon atoms in gases.

To the electron-loss cross section determined in this experiment, there corresponds a mean free path $\lambda_l = v_1\tau = (N\sigma_l)^{-1}$ for loss of correlation between the electron and the proton of given incident projectiles. It is of interest to compare the mean free path of such an electron, correlated with a moving proton, to the inelastic mean free path of a free electron injected into the solid with the same velocity. Measurements of these mean free paths λ_T, or attenuation lengths, are available in the literature for our velocity range because of their considerable importance in Auger electron spectroscopy and x-ray photoelectron spectroscopy. A compilation of these data has been pre-

TABLE I. Charge-exchange cross sections for protons in carbon as determined in this experiment, and calculated from the Brandt-Sizmann (BS) theory.

Proton energy (MeV)	σ_l^{obs} (10^{-17} cm^2)	σ_l^{BS} (10^{-17} cm^2)	σ_c^{obs} (10^{-21} cm^2)	σ_c^{BS} (10^{-21} cm^2)
1.2	3.75 ± 0.3	2.49	11.7 ± 2.2	7.33
1.8	3.1 ± 0.25	2.11	2.7 ± 0.5	1.79
2.4	2.7 ± 0.25	1.86	0.8 ± 0.15	0.63
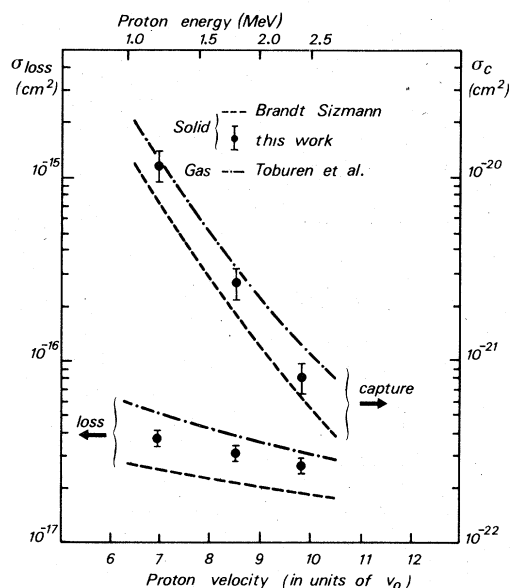
FIG. 3. Variation of charge-exchange cross sections σ_l and σ_c for protons in carbon as a function of proton velocity. Measurements from the $H^0 \rightarrow C$ experiment are compared with the Brandt-Sizmann calculations in solid carbon and the measurements reported by Toburen *et al*. (Ref. 10).

sented by Powell.[11] Figure 4 shows the variation of these various mean free paths in carbon as a function of the projectile velocity. A comparison between these values shows that the mean free path for electron loss in a solid is about three
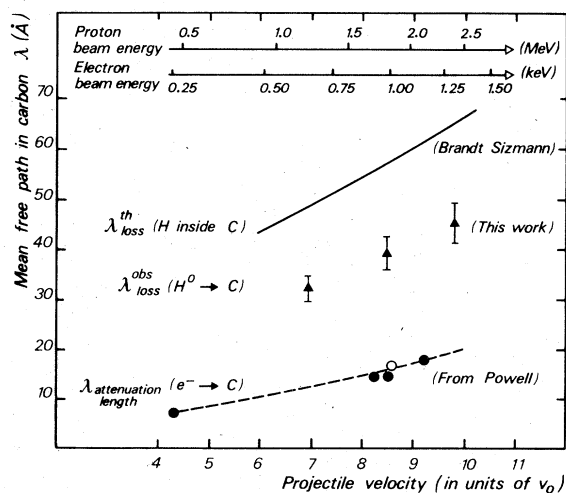
FIG. 4. Mean free paths of fast electrons in solid carbon as a function of the projectile velocity. Measurements of λ_{loss} in the $H^0 \rightarrow C$ experiment are compared with the predictions of Brandt-Sizmann for protons in carbon (solid line). Measured (closed circles) and calculated (open circle) values of the attenuation lengths corresponding to free electrons are from Ref. 11.

times longer for an electron correlated with a proton than the mean free path for inelastic collision of a free electron. This means that inside the solid an electron correlated with a moving proton has a probability of decorrelation by scattering which is lower than that of an isolated electron. The fact that our measurement of σ_l in solid carbon gives a value which is intermediate between predictions of Eq. (7) and gas phase measurements does not allow a definite conclusion about the wave function of the correlated electron within the solid; the theory of Brandt and Sizmann suppose that no bound state exists on the proton; in contrast, in the recent paper of Cross,[4] bound states on the proton are considered within the solid.

IV. NEUTRAL FRACTION WITH INCIDENT MOLECULAR BEAMS

A. Introduction

There has recently been considerable interest in the study of the interaction of fast molecular ions with solid matter.[12] Experimental evidence has been found for an increased stopping power of projectiles when they penetrate a solid as a cluster of ions.[13,14] It has been shown also that the propagation of ion clusters is strongly influenced by the wake of coherent electronic excitation trailing each ion.[15] These studies contributed significantly to the understanding of particle interactions in solids, by separating binary collisions from collective processes. The authors were stimulated by these new features of atomic collisions to undertake a systematic study of charge-exchange measurements between a fast ion cluster and a solid target to study processes leading to emission of a neutral hydrogen atom from a solid. As already mentioned, a few earlier measurements[6,7] indicated that proton clusters could produce more neutrals per incident proton than isolated protons of the same velocity.

Consider what happens when a molecular projectile enters a thin film and penetrates through it. Valence electrons are stripped off within a few atomic layers and the protons then repel each other, partly in the target and partly in the vacuum if, as for most of them, they emerge as protons. As discussed later, in our velocity range the repulsion can be considered inside the film to be purely Coulombic.

If one of the projectiles emerges as neutral, the situation is different; whatever the process of neutralization is, the repulsion inside the solid is still entirely Coulombic, but is strongly screened in the vacuum downstream from the target. This will be discussed in detail in Sec. IV E. As a consequence, the angular distribution of the neutrals

is expected to be narrower than the angular dis-
tribution of the protons.

B. Results

Neutral fractions measured with molecular pro-
jectiles are expressed in terms of the neutral
fraction Φ_0^{molec} per incident proton. The corre-
sponding value Φ_0^{atom} is measured under identical
geometrical conditions by dissociating the incident
molecular ions with a thin carbon foil placed up-
stream from the target, as described in Sec. II B.
This method provides a beam of protons with a
neutral fraction and a velocity spread which are
both negligible; the neutral fraction then mea-
sured with such a dissociated beam gives the
equilibrium neutral fraction, i.e., independent of
the target thickness, under our conditions.

The Φ_0^{molec} data, normalized to the corresponding
Φ_0^{atom} measurements, are shown in Fig. 5 as a
function of the dwell time spent by the clusters in-
side the targets. The scaling of the data with time
will be justified later.

The observed cluster effect on the neutral frac-
tion can be separated into three time ranges: (a)
For $t \gtrsim 15 \times 10^{-15}$ s, no cluster effect is observed.
(b) For 2×10^{-15} s $\lesssim t \lesssim 15 \times 10^{-15}$ s, an overproduc-
tion of neutrals is observed which diminishes
slowly with dwell time from an initial value of ~ 2
for H_3^+ and of ~ 1.5 for H_2^+. (c) For $t \lesssim 2 \times 10^{-15}$ s,
the overproduction of neutrals exhibits a very
rapid dependence upon the dwell time.

FIG. 5. Variation of $\Phi_0^{molec}/\Phi_0^{atom}$ with the projectile
dwell time for molecular beams bombarding 2–30-μg/cm^2
carbon foils, Lines correspond to the nonequilibrated
fraction as calculated from Eqs. (8) and (9).

C. Analysis of the short-dwell-time effect

The analogy between the enhancement of neutral
production observed in this time range with mole-
cular ion projectiles and the enhancement ob-
served with neutral projectiles in Sec. III is rather
easy to understand. In the case of incident neu-
trals, the effect was interpreted as the probability
that an incident atomic electron remains correla-
ted with the moving proton through the foil. In
order to estimate the corresponding probability
for the electrons of the incident molecular ions,
we consider an H_2^+ ion to be equivalent to two in-
dependent projectiles, one proton and one neutral,
and an H_3^+ ion to be equivalent to three free pro-
jectiles, one proton and two neutrals. With this
hypothesis, we can calculate the nonequilibrated
neutral fraction as a function of the projectile
dwell time in the target by using Eq. (3).

For an H_2^+ projectile, $f_0(0) = 0$ for the incident
proton and $f_0(0) = 1$ for the incident neutral. Since
$\sigma_c \ll \sigma_l$ in our energy range, the neutral yield per
incident proton becomes

$$\Phi_0^{H_2^+}(t) \sim \Phi_0(\infty) + \tfrac{1}{2}[1 - \Phi_0(\infty)]\, e^{-t/\tau}. \tag{8}$$

A similar calculation for H_3^+ gives

$$\Phi_0^{H_3^+}(t) \sim \Phi_0(\infty) + \tfrac{1}{3}[2 - \Phi_0(\infty)]e^{-t/\tau}. \tag{9}$$

After assuming that $\tau \sim \tau^{obs}$, where τ^{obs} is the
"lifetime" derived in Sec. III from the experiment
performed with incident H^0, Eqs. (8) and (9) allow
calculation of $\Phi_0^{molec}(t)$ for each projectile velocity.
Three examples of such calculations are plotted in
Fig. 5. These calculations should be compared
with the data corresponding to the fastest projec-
tiles, i.e., that of the 1.2-MeV/amu H_2^+ ions, cor-
responding to the shortest dwell times. The agree-
ment is fairly good. For molecular projectiles of
lower velocities, the thinnest targets used were
not thin enough to allow a significant observation
of this nonequilibrium effect.

In conclusion, the role played by the projectile
electron seems to explain, without any collective
effects between the projectiles in the cluster, the
overproduction of neutrals observed with molecu-
lar projectiles for very short dwell times. The
fact that this model gives a good fit of the data
when the effect is clearly observed seems to justi-
fy a posteriori the assumption that the projectile
electrons have essentially the same probability for
losing their correlation with moving protons when
they are injected as atomic electrons (H^0) or mole-
cular electrons (H_2^+, H_3^+). The cross section σ_l for
electron loss seems to be nearly the same for iso-
lated and spatially correlated protons.

For very short dwell times, the role played by
the projectile electron in the neutral production
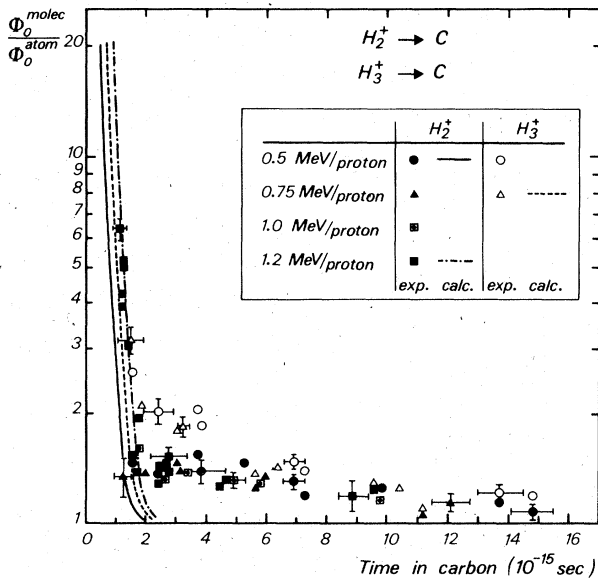
should also manifest itself by an increase of the molecular production. Measurements previously performed in our laboratory[16] of the fraction of H_2^+ molecules emerging from carbon foils bombarded with H_2^+ and H_3^+ projectiles did not concern dwell times short enough to allow clear observation of such an H_2^+ overproduction.

D. Analysis of the long-dwell-time cluster effect

Consider now proton clusters emerging from the foil with a negligible probability of correlation with the molecular electrons injected with the projectiles. The overproduction of neutrals could be caused by one or both of the following effects: (i) an increase (or a decrease) of the cross section for events leading to correlation gain (or loss) between protons and target electrons inside the solid or by (ii) an increase of the electron capture probability at the surface through which the projectile emerges.

When considering processes occurring inside the solid, it has been shown in Sec. IVC that the cross section σ_l for decorrelation is about the same for isolated protons and protons in a cluster. As for the correlation gain, it involves a scattering event with an impact parameter so small, when compared with interproton distances inside the clusters, that collective effects on it should be negligible. This must be related to measurements of forward-emitted electrons whose velocities are centered about the proton velocity. These electrons missed the capture by a proton, nevertheless their yield per proton provides information about the cross section for scattering leading to correlation. The first measurement performed by Dettmann *et al.*[17] with 100-keV/amu H^+ and H_2^+ projectiles in carbon showed that the electron yield per proton was higher by a factor of 2 with H_2^+ projectiles. More recently, Duncan and Menendez,[18] using 0.2–1.0-MeV/amu H^+ and H_2^+ projectiles in carbon, found that the electron yield is the same for both projectiles. This last measurement performed in our energy range could confirm that the cross section for scattering leading to correlation is the same for isolated protons in a cluster.

The cluster effect then should take place just after emergence from the foil, when the electron capture occurs, by increasing the capture probability of electrons which have a low probability of capture by an isolated proton. Such a collective effect depends on the distance separating the protons in a cluster as it emerges from the foil.

To calculate the emergent internuclear separation R between the protons after a dwell time t inside the target, one must have information about the initial configuration of the projectiles and the dynamics of the Coulomb repulsion inside the solid as a function of time.

For H_2^+ ion, a mean value $\overline{R}_0 \sim 1.3$ Å can be calculated[13,19] by assuming that the relative population of the vibrational levels follows the Franck-Condon principle when the molecular ions are extracted from the accelerator-ion source.

For H_3^+ ions, no simple theoretical estimate of $\overline{R}_0$ is possible. A study of this initial configuration has just been performed in our laboratory; it was concluded that protons in H_3^+ beams are ~1.2 Å apart in a triangular configuration. The description and discussion of this determination will be published elsewhere.[20]

With these initial configurations, the explosion of the proton cluster inside the target was calculated by using a nonscreened coulomb potential. This approximation is valid because the inter-proton distances considered are small when compared with the dynamic screening length v_1/ω_p, where ω_p is the plasma frequency of the target valence electrons. Furthermore, screening due to the projectile electrons can be neglected because the electron correlation path lengths are much smaller than the target thicknesses considered here. One can convert the repulsion time t inside the target into a mean internuclear separation R between the protons when they emerge from the foil as shown in Fig. 6.

Figure 7 shows the data of Fig. 5 scaled now with R, after removal of the short-dwell-time effect
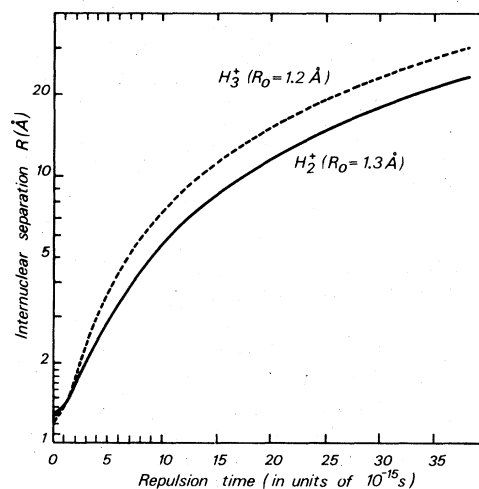
FIG. 6. Internuclear separation in a proton cluster as a function of the repulsion time. It is assumed that the coulomb force is not screened and that the initial separations are $R_0 = 1.3$ and 1.2 Å for the dicluster (solid line) and the tricluster (dashed line), respectively. These values correspond to the mean internuclear separations of the H_2^+ and H_3^+ incident projectiles.
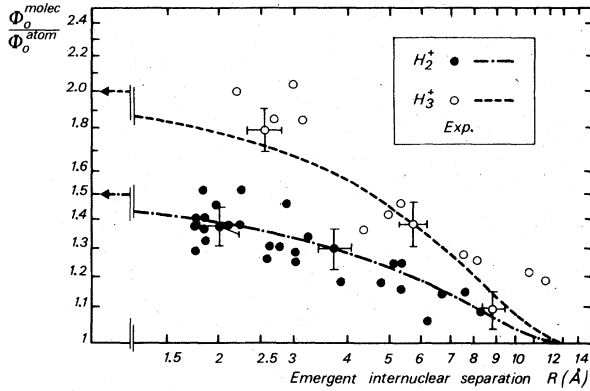
FIG. 7. Variation of $\Phi_0^{molec}/\Phi_0^{beam}$ for H_2^+ and H_3^+ projectiles as a function of the mean internuclear separation in the photon clusters when they emerge from the foil. Lines correspond to the predictions of Eqs. (14) and (15), and arrows are the limits predicted when $R \to 0$.

analyzed in Sec. IV C. The neutral production becomes normal for $R \gtrsim 15$ Å. The molecular effect is of the order of 1.5 and 2 for H_2^+ and H_3^+, respectively, for inter-proton distances of the order of the initial separations.

Some electrons can emerge from the foil with a velocity correlation with the projectiles, without contributing to formation of a neutral atom, as observed experimentally.[17,18] In the case of a proton cluster, one may consider the probability for an electron which has gained correlation with a proton to be captured by another proton of the same cluster. This probability could explain the overproduction of neutrals observed in the range of dwell times considered in this work.

We give here a tentative explanation of this effect, based on the main features of our results which are the ratio, approximately two, between the respective magnitudes of the effect for H_3^+ and H_2^+, for any value of R, and the absolute values of the effect for the smallest values of R, approximately 2 and 1.5 for H_3^+ and H_2^+, respectively.

The distance R, which will be denoted $2 R_A$, for which the effect vanishes in both cases, H_2^+ and H_3^+ is also of interest. We interpret the distance R_A by assuming that to be captured by a proton the electron must be inside a sphere, centered at the proton, with a radius R_A. We will call S_1, S_2, and S_3 the spheres associated with each proton of a cluster. A cluster effect then appears when $R < 2R_A$, i.e., when the spheres S_1, S_2, and S_3 overlap; an electron of S_1, for instance, can then be captured by protons 2 or 3. For the smallest experimental values of R, which are close to R_0, the overlap can be considered total since R_0 is much smaller than R_A.

We are led to postulate that a proton, upon emer-

gence from a solid, can be accompanied by electrons of two kinds; first it has a probability n_1 of being accompanied by an electron, the capture probability of which is unity; second it has a probability n_2 of being accompanied by an electron, the mean capture probability of which is K, with $K \ll 1$. The neutral fraction of a transmitted beam from incident protons is then

$$\Phi_0^{H^+} = n_1 + Kn_2 . \tag{10}$$

It is clear that the cluster effect does not change the contribution of the electrons of the first group since they are always captured but will be due to those of the second group, which are assumed to be uniformly distributed inside the sphere of radius R_A.

Then, if V_c is the volume common to spheres S_1 and S_2 (expressed in units of the volume of each sphere), the neutral fraction from an incident beam of H_2^+ ions can be written

$$\Phi_0^{H_2^+} = n_1 + Kn_2(1 - V_c) + K(2n_2)V_c , \tag{11}$$

$$\Phi_0^{H_2^+} = \Phi_0^{H^+} + Kn_2V_c .$$

In the same way, $\Phi_0^{H_3^+}$ can be written, V_{cc} being the volume common to three equidistant spheres:

$$\Phi_0^{H_3^+} = n_1 + Kn_2(1 - 2V_c + V_{cc})$$
$$+ K(2n_2)(2V_c - 2V_{cc}) + K(3n_2)V_{cc} ,$$

or

$$\Phi_0^{H_3^+} = \Phi_0^{H^+} + 2Kn_2V_c . \tag{12}$$

An immediate result retrieved by Eqs. (11) and (12) is that the H_3^+ effect is twice the H_2^+ effect. If now one imposes the experimental values 1.5 and 2 for zero thickness ($R \to R_0$, $V_c \to 1$) one obtains

$$Kn_2 = \tfrac{1}{2} \Phi_0^{H^+} . \tag{13}$$

Using (13), (11), and (12) can be rewritten

$$\Phi_0^{H_2^+}/\Phi_0^{H^+} = 1 + \tfrac{1}{2} V_c , \tag{14}$$

$$\Phi_0^{H_3^+}/\Phi_0^{H^+} = 1 + V_c . \tag{15}$$

The variation of the neutral fraction in function of R, as given by Eqs. (14) and (15) are shown in Fig. 7 (solid lines). The agreement with the experimental data is not too surprising since the calculation takes the main features of the experimental results into account.

Interesting conclusions can be drawn from this model, which is the only one with which both H_2^+ and H_3^+ data can be explained.

First, the condition $K \ll 1$ is dictated by the experimental evidence that the H_3^+ effect is twice the H_2^+ effect for any value of R. Indeed, if this condition were not fulfilled, there would be a saturation when passing from the H_2^+ to the H_3^+ case.

The magnitude of the cluster effect leads us, by means of (10) and (13) to conclude that

$$n_1 \sim K n_2. \tag{16}$$

Equation (16) implies that for an atomic projectile the contribution of the two kinds of electrons defined above are nearly equal. Those electrons of the first kind appeared to be strongly correlated to a proton when emerging (a bound state, as suggested by Cross,[4] would be the extreme degree of correlation). The number of electrons of the second kind is much higher (probabilities n_1 and n_2 are related by $n_1/n_2 = K$); they could be electrons which have lost correlation a few atomic layers before emergence. Our data and our interpretation suggest that they play an important role in the neutralization process.

Moreover, it is tempting to mention the similarity between these data and the well-known partition between the two processes of electronic energy loss of charged particles in solids, binary collisions and collective excitations, which were also separated in molecular beam experiments.[13]

There is another way to consider this effect: it has been shown[16,21] that cluster protons emerging from solids have a probability of producing an H_2^+ molecular ion which is small, and rapidly decreasing with R. If electron capture into a stable molecule is possible, it might be assumed that capture into an unstable molecule is also possible. Such a capture would lead to a final state of one proton plus a neutral atom. Formation of a repulsive molecular state could then be the process producing extra neutrals when the incident projectiles are molecular ions.

In fact, both models have the common concept of an electron being initially correlated with one proton and finally captured by another proton of the same cluster. Our calculation is simple enough to accept both interpretations. Repulsive molecular states will be considered again in the next section.

The last point concerns the meaning of the radius R_A, which is of the order of 7 Å. R_A could be characteristic of the bulk of the target (the screening distance is, perhaps fortuitously of the order of 7 Å in carbon in our energy range) but we rather believe that it is characteristic of the neutral atom produced (whether via a molecular state or not). Similar experiments performed at higher velocities (with a correspondingly higher screening distance) or with another material could discriminate between these two interpretations.

E. Angular distributions of neutrals

The angular distributions of neutrals and charged particles emerging from carbon foils were mea-
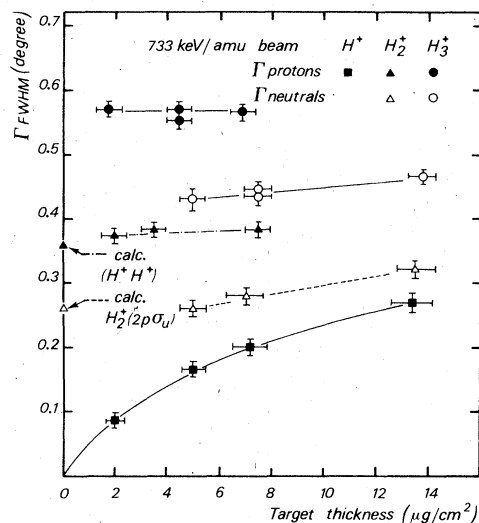
FIG. 8. Variation of the FWHM of the angular distributions of protons and neutrals emerging from carbon foils as a function of the target thickness. Foils are bombarded with 733-keV/amu H^+, H_2^+, and H_3^+ projectiles. Lines drawn through each set of data are to guide the eye. Arrows correspond to the zero thickness prediction of the widths of the proton distribution (▲) and of the neutral distribution (△) resulting from the explosion of a free (H^+ H^+) pair and a repulsive (H^+ H^0) $2p\,\sigma_u$ molecule. Both clusters are assumed to be randomly oriented with a distribution of internuclear distances identical to the distribution of the incident H_2^+ projectiles.

sured with the experimental method described in Sec. II C. Measurements of these angular widths were first motivated by the need for well-determined geometrical conditions for neutral fraction measurements, but it also appeared that this study was relevant to the understanding of electron capture by a proton cluster because the angular distributions of neutrals are determined by the internal energy of the (electron-proton cluster) system as it emerges from the foil.

Figure 8 shows proton and neutral angular widths $\Gamma_{\rm FWHM}$ (full width at half-maximum) for carbon targets of various thicknesses bombarded with 733-keV/amu H^+, H_2^+, and H_3^+ projectiles. As expected the angular widths are narrower for the neutral

TABLE II. Angular widths of the neutral and charged fractions emerging from a 5-μg/cm^2 carbon foil bombarded with 733-keV/amu H^+, H_2^+, and H_3^+ projectiles.

Angular widths $\Gamma_{\rm FWHM}$ (deg)	Incident projectiles		
	H^+	H_2^+	H_3^+
Protons	0.085 ± 0.01	0.38 ± 0.01	0.57 ± 0.02
Neutrals		0.26 ± 0.01	0.43 ± 0.02

component than for the charged component when the projectiles are molecular ions. Table II gives these relative widths when 733-keV/amu projectiles bombard a 5-μg/cm^2 carbon foil. As also expected, with an incident proton beam the neutral and charged components exhibit the same width.

The thickness dependence of the widths is governed by the multiple scattering of the projectiles inside the target and by the relative amounts of the cluster explosion occurring inside and outside the target.

In the H$_2^+$ case, if one neglects repulsion inside the target, one can estimate the widths of the neutral and the charged distributions by comparing the explosion of a diproton cluster and of a (proton-neutral) cluster. As suggested in Sec. IV D, the exploding (proton-neutral) cluster could be described as an excited H$_2^+$ molecule in a repulsive state. Excited molecular states dissociate into a proton and a hydrogen atom, as seen in Fig. 9. For instance,

$$H_2^+(3s\,\sigma_g) \rightarrow H^+ + H^0(3s),$$

$$H_2^+(2p\,\pi_u) \rightarrow H^+ + H^0(2p).$$
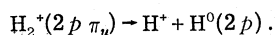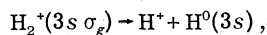
The only excited state leading to a hydrogen atom in the ground state is

$$H_2^+(2p\,\sigma_u) \rightarrow H^+ + H^0(1s).$$
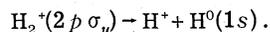
For a given initial interproton separation, the amount of internal energy liberated from a diproton cluster can be directly compared with the internal energy liberated from such a repulsive molecule, as shown in Fig. 9 by the vertical arrows for a $2p\,\sigma_u$ state.

To go further in this analysis, one has to consider the relative population of these numerous excited molecular states. Beam-foil measurements give information describing the final relative populations of the excited neutral atoms; Bukow et al.[22] compared these populations by bombarding carbon foils with 50–400-keV H$_2^+$ and proton beams. Their conclusion is that the population of levels of higher angular momentum is larger with H$_2^+$ than with H$^+$ projectiles. They also observe that with both projectiles the population decreases as n^{-3}, where n is the principal quantum number. Most of the hydrogen atoms are in the ground state.

In our experiment it is then reasonable to assume that if intermediate molecular states are involved, the $2p\,\sigma_u$ state should be the most populated because it leads to a hydrogen atom in its ground state.

The relative amount of kinetic energy released from the diproton (H$^+$ + H$^+$) and the (H$_2^+$) $2p\,\sigma_u$ state, can be estimated in the limit in which the targets
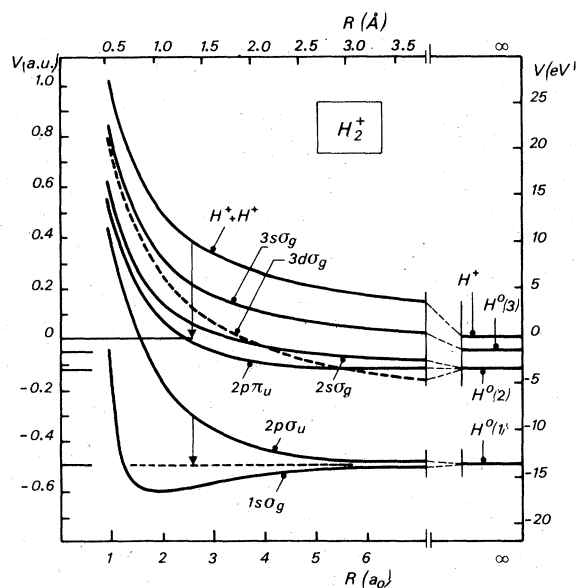
FIG. 9. Potential energy curves for the proton dicluster as free protons (H$^+$ + H$^+$), as molecular ions (H$_2^+$) in the 1s σ_g ground state, and as repulsive molecules in various excited states of the H$_2^+$ ion. Also indicated are the final states of resulting hydrogen atoms after complete explosion of the dicluster. Vertical arrows show the relative amount of kinetic energy released from (H$^+$ H$^+$) and from (H$_2^+$) $2p\,\sigma_u$ clusters exploding from a given internuclear separation.

are so thin that multiple scattering effects are negligible and the internuclear distributions are nearly the same in the emergent and incident clusters. To an initial interproton distance R_0 corresponds a potential energy E^+ for the diproton cluster and E^0 for the H$_2^+(2p\,\sigma_u)$ molecular ion. If these clusters are both randomly oriented, the distributions of partners after repulsion have respective widths $\Gamma^+(R_0) \propto (E^+)^{1/2}$ and $\Gamma^0(R_0) \propto (E^0)^{1/2}$.

For a given distribution $N(R_0)$ of initial interproton distances, one can simulate the measured angular distributions by integrating these distributions over $N(R_0)$.

The result of such a calculation is shown in Fig. 8 for 733-keV/amu H$_2^+$ ions. It gives $\Gamma^+ = 0.36°$ for a diproton cluster and $\Gamma^0 = 0.26°$ for a H$^+$ H$^0(2p\,\sigma_u)$ cluster. The distribution $N(R_0)$ was calculated by assuming that the population of H$_2^+(1s\,\sigma_g)$ vibrational levels follows the Franck-Condon principle.[19] A comparison between such an estimate of the relative widths in the limiting case of a zero thickness target and the data does not allow a definite conclusion but shows that our results seem compatible with the formation of an excited molecular state when neutral atoms are produced from a dicluster. Such an intermediate

molecular state could explain both atomic excitation and angular distribution of the observed neutral atoms.

In the case of a tricluster, no simple calculation can be performed because information on H_3^{++} is not available. Nevertheless, a similar molecular stage is likely if one considers the similarity between H_3^+ and H_2^+ data. Such a similarity between dicluster and tricluster behavior has been previously shown by studying the relative probability of producing an H_2^+ bound state from H_2^+ and H_3^+ projectiles in the energy and thickness range of this work.[16]

As a final comment on these cluster effects on charge-exchange processes of fast hydrogen ions in solids, we would like to mention another characteristic of the molecular ion-foil interaction which has been reported by Duncan and Menendez[18]: the cusp-shaped peak of electrons emerging from the foil close to the beam direction is narrower when H_2^+ projectiles are used. This effect, which has been recently confirmed by Meckbach *et al*.,[23] is clearly related to our study but at this point our model is unable to explain this curious feature.

V. CONCLUSION

The nonequilibrated neutral fractions observed when thin carbon foils are bombarded with fast hydrogen atoms provide a direct measurement of the charge-exchange cross sections for fast protons in solids. In the MeV energy range, the measured cross sections in solid and gas targets are found to agree quite closely. However, this result, obtained for carbon targets only, does not make more evident the neutralization process itself. Particularly, it does not prove the presence or the absence of bound states inside the solid.

The overproduction of neutrals observed when a foil is bombarded with molecular projectiles clearly exhibits two different effects that could be called surface and solid effects.

The solid effect, observed for very short dwell times, is the charge equilibration of the projectiles as they penetrate deeper into the solid. Our measurements show that the approach to equilibrium follows essentially the same law for H^0, H_2^+, and H_3^+ projectiles.

The surface effect emerges at longer dwell times in the foil and has been interpreted as an interference between the contributions of the protons in a cluster in the successive phases of a multistep process; namely, a collision leading to a correlation of the electron-proton pair and to a final capture at the exit surface of the foil, as proposed by Brandt and Sizmann. We are led to conclude that this effect concerns only a fraction of emitted electrons, perhaps those which have lost their correlation inside the target.

Finally, we have related the angular distribution of neutral atoms produced from a proton cluster to the electronic configuration of the unstable electron-cluster system created upon emergence from the foil. In the case of diproton clusters, these distributions are compatible with an intermediate capture into an H_2^+ ($2p\,\sigma_u$) state which leads to the formation of a neutral atom in the ground state. To obtain accurate information bearing upon a possible anisotropy of this molecule in a repulsive state, more detailed experiments and analysis will be necessary.

*Present address: Physics Division, Argonne National Lab., Argonne, Ill. 60439.

[1]A. Chateau-Thierry, A. Gladieux, and B. Delaunay, Nucl. Instrum. Methods 132, 553 (1976).

[2]M. J. Gaillard, J. C. Poizat, J. Remillieux, A. Chateau-Thierry, A. Gladieux, and W. Brandt, Nucl. Instrum. Methods 132, 547 (1976).

[3]W. Brandt and R. Sizmann, in *Atomic Collisions in Solids* (Plenum, New York, 1975), Vol. 1, p. 305; and unpublished.

[4]M. C. Cross, Phys. Rev. B 15, 602 (1977).

[5]W. Brandt, in Ref. 3, Vol. 1, p. 261.

[6]B. T. Meggitt, K. G. Harrison, and M. W. Lucas, J. Phys. B 6, L 362 (1973).

[7]A. Chateau-Thierry and A. Gladieux (private communication).

[8]E. F. Kennedy, D. H. Youngblood, and A. E. Blaugrund, Phys. Rev. 158, 897 (1967).

[9]S. Datz, F. W. Martin, C. D. Moak, B. R. Appleton, and L. B. Bridwell, Radiat. Eff. 12, 163 (1972).

[10]L. H. Toburen, M. Y. Nakai, and R. A. Langley, Phys. Rev. 171, 114 (1968).

[11]C. J. Powell, Surf. Sci. 44, 29 (1974).

[12]See, for instance, W. Brandt and R. Ritchie, Nucl. Instrum. Methods 132, 43 (1976), and references therein.

[13]W. Brandt, A. Ratkowski, and R. H. Ritchie, Phys. Rev. Lett. 33, 1325 (1974).

[14]J. W. Tape, W. M. Gibson, J. Remillieux, R. Laubert, and H. E. Wegner, Nucl. Instrum. Methods 132, 75 (1976).

[15]D. S. Gemmell, J. Remillieux, J. C. Poizat, M. J.

Gaillard, R. E. Holland, and Z. Vager, Nucl. Instrum. Methods 132, 61 (1976).

[16]M. J. Gaillard, J. C. Poizat, A. Ratkowski, and J. Remillieux, Nucl. Instrum. Methods 132, 69 (1976).

[17]K. Dettmann, K. G. Harrison, and M. W. Lucas, J. Phys. B 7, 269 (1974).

[18]M. M. Duncan and M. G. Menendez, Phys. Rev. A 13, 566 (1976).

[19]J. Remillieux, in Radiation Research (Academic, New York, 1975), p. 302.

[20]M. J. Gaillard, J. C. Poizat, A. Ratkowski, and J. Remillieux (unpublished).

[21]W. Brandt, R. Laubert, and A. Ratkowski, Nucl. Instrum. Methods 132, 57 (1976).

[22]H. H. Bukow, H. V. Buttlar, D. Haas, P. H. Heckmann, M. Holl, W. Schlagheck, D. Schurmann, R. Tielert, and R. Woodruff, Nucl. Instrum. Methods 110, 89 (1973).

[23]W. Meckbach, K. C. R. Chiu, H. Brongersma, and J. Wm. McGowan (unpublished).